AD-A186 884 THE USE OF THE DIRECT MEASUREMENT OF SOLAR RADIATION FOR THE DETERMINATIO..(U) CHEMICAL RESEARCH DEVELOPMENT AND ENGINEERING CENTER ABERDEEN.. M M MYIRSKI JUL 87 1/1

UNCLASSIFIED CRDEC-TR-87065 F/G 3/2 NL

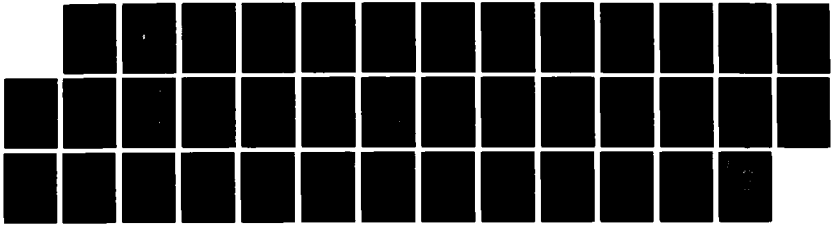

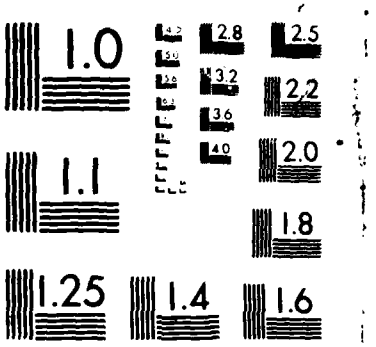

(12)

CHEMICAL RESEARCH, DEVELOPMENT & ENGINEERING CENTER



CRDEC-TR-87065

# THE USE OF THE DIRECT MEASUREMENT OF SOLAR RADIATION FOR THE DETERMINATION OF PASQUILL STABILITY PARAMETER



by Michael M. Myirski
STUDIES AND ANALYSIS OFFICE

July 1987



U.S. ARMY ARMAMENT MUNITIONS CHEMICAL COMMAND

Aberdeen Proving Ground, Maryland 21010-5423

UNCLASSIFIED

SECURITY CLASSIFICATION OF THIS PAGE

# REPORT DOCUMENTATION PAGE

| | |
|---|---|
| 1a. REPORT SECURITY CLASSIFICATION<br>UNCLASSIFIED | 1b. RESTRICTIVE MARKINGS |
| 2a. SECURITY CLASSIFICATION AUTHORITY | 3. DISTRIBUTION / AVAILABILITY OF REPORT<br>Approved for public release; distribution is unlimited. |
| 2b. DECLASSIFICATION / DOWNGRADING SCHEDULE | |
| 4. PERFORMING ORGANIZATION REPORT NUMBER(S)<br>CRDEC-TR-87065 | 5. MONITORING ORGANIZATION REPORT NUMBER(S) |
| 6a. NAME OF PERFORMING ORGANIZATION<br>CRDEC<br>6b. OFFICE SYMBOL (If applicable)<br>SMCCR-ST | 7a. NAME OF MONITORING ORGANIZATION |
| 6c. ADDRESS (City, State, and ZIP Code)<br>Aberdeen Proving Ground, MD 21010-5423 | 7b. ADDRESS (City, State, and ZIP Code) |
| 8a. NAME OF FUNDING / SPONSORING ORGANIZATION<br>CRDEC<br>8b. OFFICE SYMBOL (If applicable)<br>SMCCR-ST | 9. PROCUREMENT INSTRUMENT IDENTIFICATION NUMBER |
| 8c. ADDRESS (City, State, and ZIP Code)<br>Aberdeen Proving Ground, MD 21010-5423 | 10. SOURCE OF FUNDING NUMBERS<br>PROGRAM ELEMENT NO.: <br>PROJECT NO: 1L162706<br>TASK NO: A553<br>WORK UNIT ACCESSION NO: |
| 11. TITLE (Include Security Classification)<br>The Use of the Direct Measurement of Solar Radiation for the Determination of Pasquill Stability Parameter | |
| 12. PERSONAL AUTHOR(S)<br>Myirski, Michael M. | |
| 13a. TYPE OF REPORT<br>Technical<br>13b. TIME COVERED<br>FROM 84 Jan TO 84 Aug<br>14. DATE OF REPORT (Year, Month, Day)<br>1987 July<br>15. PAGE COUNT<br>37 | |
| 16. SUPPLEMENTARY NOTATION | |

| 17. COSATI CODES | | |
|---|---|---|
| FIELD | GROUP | SUB-GROUP |
| 15 | 06 | 03 |
| | | |

18. SUBJECT TERMS (Continue on reverse if necessary and identify by block number)
Solar radiation
Atmospheric stability
Pasquill-Turner stability
Smith Algorithm
Insolation parameter $\Phi$

19. ABSTRACT (Continue on reverse if necessary and identify by block number)

Two schemes for estimating the amount of solar radiation received at the earth's surface are compared to solar radiation measurements. These measurements were made by the Atmospheric Sciences Laboratory Meteorological Team at Aberdeen Proving Ground during the months of July and December 1983 and February and March 1984. This data was acquired over a total of 25 days and from 214 individual observations. These observations were grouped into both instantaneous and hourly averaged data.

Of the two schemes studied, the insolation parameter $\Phi$ performed better than the net radiation index used in the Pasquill-Turner Stability Category algorithm.

To eliminate the need to subjectively estimate the amount of solar radiation, an algorithm is presented to determine a continuous Pasquill Stability Parameter based on

(Continued on reverse)

| | |
|---|---|
| 20. DISTRIBUTION / AVAILABILITY OF ABSTRACT<br>☒ UNCLASSIFIED/UNLIMITED ☐ SAME AS RPT ☐ DTIC USERS | 21. ABSTRACT SECURITY CLASSIFICATION<br>UNCLASSIFIED |
| 22a. NAME OF RESPONSIBLE INDIVIDUAL<br>TIMOTHY E. HAMPTON | 22b. TELEPHONE (Include Area Code)<br>(301) 671-2914<br>22c. OFFICE SYMBOL<br>SMCCR-SPS-T |

DD FORM 1473, 84 MAR 83 APR edition may be used until exhausted
All other editions are obsolete

SECURITY CLASSIFICATION OF THIS PAGE
UNCLASSIFIED

19. ABSTRACT (Continued)

direct measurement of solar radiation. This algorithm compares favorably to one previously developed by ~~Smith of~~ Great Britian's meteorological office.

## PREFACE

The work described in this report was authorized under Project No. 1L162706A553, CB Defense and General Investigations, Technical Area 3-B, Analysis and Integration of Chemical Defense Systems. This work was started in January 1984 and completed in August 1985.

The use of trade names or manufacturers' names in this report does not constitute an official endorsement of any commercial products. This report may not be cited for purposes of advertisement.



This report has been approved for release to the public.

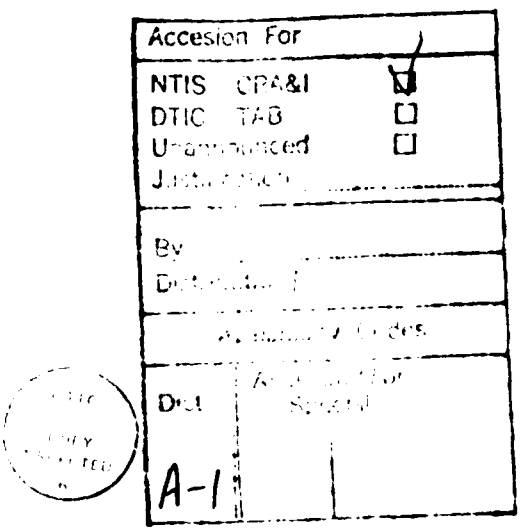

Blank

CONTENTS


| | | Page |
|---|---|---|
| 1. | OBJECTIVE | 7 |
| 2. | BACKGROUND | 7 |
| 3. | SOLAR RADIATION | 8 |
| 4. | PASQUILL-TURNER STABILITY CATEGORY | 9 |
| 5. | DATA COLLECTION | 9 |
| 6. | SAMPLE INSOLATION MEASUREMENTS | 13 |
| 7. | DATA SUMMARY - NET RADIATION | 13 |
| 8. | DATA COMPARISON - INSOLATION PARAMETER $\Phi$ | 16 |
| 9. | DATA COMPARISON - SMITH ALGORITHM | 30 |
| 10. | CONCLUSIONS | 34 |
| 11. | RECOMMENDATIONS | 35 |
| | LITERATURE CITED | 37 |

Blank

# THE USE OF THE DIRECT MEASUREMENT OF SOLAR RADIATION FOR THE DETERMINATION OF PASQUILL STABILITY PARAMETER

## 1. OBJECTIVE

My objectives were to compare two schemes for estimating the amount of solar radiation received at the earth's surface with solar radiation measurements and to develop an algorithm to determine the Pasquill Stability Parameter based on direct measurements of solar radiation.

## 2. BACKGROUND

Many organizations, including the U.S. Army, have a keen interest in the rates of dispersion for vapors, aerosols, and smokes introduced to the atmosphere. These dispersion rates are needed to predict the downwind concentrations of these substances. Before such estimates can be made, however, atmospheric turbulence must be understood and categorized.

Atmospheric turbulence is the key parameter in predicting concentration levels. It arises from two physical phenomena, solar radiaction and wind. Solar radiation creates atmospheric turbulence because the atmosphere and the earth's surface absorb heat at different rates. Due to its physical properties, the earth's surface absorbs heat much more quickly than the atmosphere. This excess heat is transferred to the air in contact with the surface, which in turn transfers heat to the layers of the air above it. This process transfers properties of the lowest air layers to those above through mixing, or atmospheric turbulence. At night, the surface cools faster and the process reverses itself.

The wind also creates the mixing of air layers. As it drags along the (uneven) surface, the wind creates small whirlwinds, or eddies, that have the same effect on mixing as does solar radiation. As the wind increases, so does the level of mixing. Therefore, to estimate the dispersion rates of chemicals released into the atmosphere, the combined effects of solar radiation and wind on atmospheric turbulence must be determined.

The Pasquill Stability Category as revised by Turner,[1] is a popular method for characterizing turbulence from the combined effects of solar radiation and wind. An important assumption in this procedure is that the radiation reaching the earth's surface can be determined through knowledge of solar altitude, cloud cover, and cloud height. Cloud height is an important consideration because higher clouds allow more radiation through than the lower, denser clouds. Solar altitude can be determined precisely assuming a knowledge of latitude, longitude, date and time. However, both cloud cover and cloud height require subjective estimates. If direct measurement of solar radiation is used, the need to estimate these parameters would be eliminated.

Routine meteorological observations and solar radiation measurements have been collected. The solar radiation measurements were compared with subjective estimates of the same quantity, and a system to determine the Pasquill Stability Parameter based on direct measurement of solar radiation is included.

## 3. SOLAR RADIATION

The energy in the form of solar radiation received at the top of the earth's atmosphere varies ver. little; the sun supplies a fairly constant amount. The so-called solar constant averages 1340 watts per meter squared, or 1.94 langleys (ly) per minute. The solar constant is defined as the solar radiation at normal incidence (90°) outside the atmosphere at the mean solar distance (average distance between the sun and earth). This quantity fluctuates as much as ± 1.5%, while the varying distances between the sun and earth produce changes on the order of ± 3.5% from the mean value.[2] However, solar radiation does not travel unimpeded through the atmosphere. The radiant energy received at the earth's surface, which determines atmospheric turbulence and stability, varies tremendously from place to place.

The amount of radiation received at the surface is dependent on several factors, including latitude, time of day, cloudiness, atmospheric pollutants, and surface type. Both latitude and time of day determine the angle at which the solar radiation strikes the surface (radiation increases as the angle increases).

Cloudiness and atmospheric pollutants absorb, reflect, and scatter solar radiation. Absorption is the process whereby solar radiation is taken in. Reflection involves the change in direction of the solar radiation after striking a surface, such as a water droplet in a cloud. Scattering is the mechanism where solar radiation is separated and dispersed in many directions.

Surface type is instrumental in determining the amount of radiation reflected. For instance, snow and ice reflect much more radiation than a forest-covered surface. Table 1 shows the approximate effects the atmosphere has on solar radiation.

Table 1. Solar Radiation Lost to the Atmosphere

| Percentage lost | Reason |
|---|---|
| 20 | Absorbed by atmosphere and clouds |
| 22 | Reflected by clouds |
| 5 | Scattered by atmosphere |
| 3 | Reflected by earth's surface |
| Total 50 | |

Thus, only 50% of the radiation reaching the top of the atmosphere is received by the earth's surface. The radiation absorbed by a surface unimpeded by any of these processes is referred to as direct radiation. The radiation reaching a surface as a result of scattering or reflection from another surface is called diffuse radiation. It is interesting to note that the solar radiation reaching the earth's surface can actually exceed the solar constant. If the sun is nearly directly overhead and the sky clear and clean, very little radiation will be absorbed by the atmosphere. And if some bright, fair-weather cumulus clouds are around, they may add significant

contributions from the radiation they reflect. Thus, when diffuse radiation is considered, the earth's surface may actually receive more radiation than the top of the atmosphere directly above.

## 4. PASQUILL-TURNER STABILITY CATEGORY

Tables 2 and 3 are used to determine the Pasquill Stability Category, i.e., relative atmospheric turbulence. From the existing meteorological conditions, determine the amount of the sky obscured by clouds, the approximate cloud height,* and the angle of the sun above the horizon. Use Table 2 to determine the net radiation index (NRI). Note that the index ranges from 0 to 4 during the day and -2 to 0 during the night. This index reflects the relative amount of solar radiation reaching the earth's surface under the existing meteorological conditions. The negative net radiation indices during the night reflect the transfer of heat away from the surface.

Finally, the net radiation index determined above is used with the wind speed to find the Pasquill Stability Category, ranging from very unstable (A) to very stable (F), in Table 3. Tables 2 and 3 summarize the effects of solar radiation and wind on the classification of atmospheric turbulence.

Some interesting aspects follow from a study of Tables 2 and 3. For a given NRI, increasing the wind speed increases the likelihood that the stability will be D (neutral). For a given wind speed, increasing the NRI creates more unstable atmospheric conditions. The greatest range of stabilities occurs at the lowest wind speeds. Stabilities A, B, and C can only occur during the daytime; Stabilities E and F occur only at night; and Stability D can occur anytime. In fact, Stability D is the most common atmospheric condition.

## 5. DATA COLLECTION

The U.S. Army Atmospheric Sciences Laboratory (ASL) has many small, specialized meteorological teams located throughout the country, including a station near Phillips Airfield at Aberdeen Proving Ground (APG), Maryland. The team routinely collects meteorological data and provides forecasts for various Army elements at APG.

Between the hours of 8:00 a.m and 4:00 p.m, Monday through Friday, the meteorological team routinely collects such data as temperature, dew point, pressure, wind speed and direction, relative humidity, visibility, precipitation, cloud cover, and cloud height. At my request, the team also measured solar radiation.

---

*Since cloud types are confined to certain levels in the atmosphere, cloud height can be approximated reliably through a knowledge of cloud types. For example, see Cloud Charts, Inc. Copyright 1958.

Table 2. Net Radiation Index

| Cloud cover (1/8) | Day | | | | | | Night* | | | |
|---|---|---|---|---|---|---|---|---|---|---|
| | 0-4 | 5-7 | | | 8 | | 8 | | 7-4 | 3-0 |
| Cloud height (1000 ft) | | >16 | 16-7 | <7 | >7 | <7 | <7 | >7 | | |
| Solar altitude | | | | | | | | | | |
| <15° | 1 | 1 | 1 | 1 | 1 | 0 | 0 | -1 | -1 | -2 |
| 15-35° | 2 | 2 | 1 | 1 | 1 | 0 | | | | |
| 35-60° | 3 | 3 | 2 | 1 | 2 | 0 | | | | |
| >60° | 4 | 4 | 3 | 2 | 3 | 0 | | | | |

*Night is defined as the period from 1 hour before sunset to 1 hour after sunrise.

Table 3. Pasquill Stability Category as a Function of Net Radiation Index and Windspeed

| Windspeed m/sec | Net radiation index | | | | | | |
|---|---|---|---|---|---|---|---|
| | 4 | 3 | 2 | 1 | 0 | -1 | -2 |
| <1 | A | A | B | C | D | F | F |
| 1 | A | B | B | C | D | F | F |
| 2 | A | B | C | D | D | E | F |
| 3 | B | B | C | D | D | E | F |
| 4 | B | C | C | D | D | D | E |
| 5 | C | C | D | D | D | D | E |
| 6 | C | C | D | D | D | D | D |
| >6 | C | D | D | D | D | D | D |

APG is located in northeastern Maryland on two separate peninsulas in the northern section of the Chesepeake Bay. The one-story meteorological building is located approximately 50 meters from the waterfront. The terrain rises away from the immediate area of the building; i.e., the building and instruments nearby are located in a localized low spot. In addition, trees and other buildings almost completely surround the meteorological instrumentation area. These geographical considerations no doubt affect some of the meteorological data collected, particularly wind speed and direction.

Surface observations of the meteorological parameters are recorded between 5 minutes before and the top of each hour. All observations are made in accordance with the established federal guidelines.[3] The data are recorded on forms MF1-10A and MF1-10B for national quality control and archiving, respectively. For this study, the meteorological parameters of most interest are wind speed, cloud cover, cloud height, and solar radiation. The solar elevation will also be required, but these can be determined mathematically.

Wind speed was recorded using a Belfort T420 anemometer perched atop the meteorological building, approximately 10 meters above ground. Wind speeds are listed in miles per hour and represent 1-minute averages. In subsequent conversations with specialists from the meteorological team, the wind speed measurements are not expected to be representative of the general area. They feel that the wind speed measurements recorded are lower than should be expected because the instrumentation area is lower than its surrounding and the equipment was probably sheltered by the buildings and trees and, in addition, the anemometer may not have been properly calibrated.*

Cloud cover and cloud height are measured subjectively. Cloud cover is simply the amount of sky obscured by clouds.

A meteorological specialist records cloudiness through one of four descriptors: clear, scattered, broken, or overcast. The amount of cloudiness assigned to each category is given in Table 4.

Table 4. Cloudiness Categories

| Sky description | Cloudiness amount* |
|---|---|
| Clear | 0 |
| Scattered | 3 |
| Broken | 6 |
| Overcast | 8 |

*Scale of 0-8

*Personal conversation with Mr. Paul Sisson, 10 August 1984.

Cloud height can be determined quite accurately through a knowledge of the cloud type. In general, cloud types are confined to certain layers of the atmosphere. A ceilometer is located at Phillips Airfield, but the instrument is not often used. Also, on some occasions, balloons with known ascension rates are released that can determine cloud heights. But, for the most part, cloud heights are estimated according to cloud types. Cloud heights are recorded in hundreds of feet.

Solar radiation was measured employing a glass-domed Eppley pyranometer mounted 1 meter off the ground. The device is located approximately 5 meters from the meteorological building and is connected to it by a ground cable. Solar radiation measurements are continuously recorded inside the building with a pen, strip chart, and rotating drum.

The pyranometer measures, in langleys per minute, both direct and diffuse radiation, i.e., all the radiation being received at that point.

The measurement of solar radiation was begun in June 1983. Some problems were encountered in the initial weeks of data collection. The pen used to record the radiation on the strip chart was often unreliable, including printing so wide that the chart was unreadable. This was corrected by the end of June. Only data through March 1984 judged to be very good quality was selected for this study. The dates chosen are listed in Table 5.

Table 5. Dates Selected for Data Analysis

| Month/Year | Dates |
|---|---|
| July 1983 | 1, 5, 6, 7, 8, 18, 19, 20, 21, 22 |
| December 1983 | 14, 15, 16, 19, 20, 21, 22 |
| February 1984 | 14, 15, 16, 17 |
| March 1984 | 6, 7, 8, 9 |

The solar radiation measurements received in the form of strip charts were not directly usable; the data had to be "reduced" before any analysis could begin. As mentioned previously, the strip chart provides a continuous measurement of solar radiation. Beginning at the top of each hour, a subjective estimate of the solar radiation was recorded every 5 minutes; i.e., an average value for every 5-minute increment was chosen to represent the solar radiation strength over that time interval. In addition, hourly averages were computed using these 5-minute averages. For each hourly average, the twelve 5-minute averages were given equal weights; i.e., the 12 averages were added and then divided by 12.

Table 5 represents a total of 25 days and 214 individual observations of data. This amount was judged large enough to evaluate the various solar radiation estimators used in this study.

## 6. SAMPLE INSOLATION MEASUREMENTS

Figure 1 lists the solar radiation measurements for two dates, 7 July and 21 December 1983. These dates were selected to show the seasonal differences that can be expected at APG. Table 6 shows that 7 July was a mostly sunny summer day, while 21 December was a mostly cloudy winter day.

Table 6. Sky Conditions at Aberdeen Proving Ground on Select Dates

| 7 July 1983 Cloud heights (ft)/cloud cover* | | 21 December 1983 Cloud heights (ft)/cloud cover* | | | |
|---|---|---|---|---|---|
| 8 a.m | Clear | 8 a.m | 12,000 (3) | 25,000 (3) | |
| 9 a.m | Clear | 9 a.m | 6,000 (3) | 12,000 (6) | 25,000 (6) |
| 10 a.m | Clear | 10 a.m | 12,000 (3) | 15,000 (6) | 20,000 (6) |
| 11 a.m | Clear | 11 a.m | 8,000 (3) | 12,000 (3) | 15,000 (6) |
| 12 a.m | Clear | 12 a.m | 6,000 (3) | 12,000 (6) | 20,000 (8) |
| 1 p.m | 36,000 (3) | 1 p.m | 6,000 (3) | 10,000 (8) | |
| 2 p.m | 40,000 (3) | 2 p.m | 6,000 (3) | 10,000 (8) | |
| 3 p.m | Clear | 3 p.m | 6,000 (3) | 10,000 (8) | |
| 4 p.m | Clear | 4 p.m | 6,000 (3) | 8,000 (8) | |

*Scale of 0-8

The characteristic most evident in Figure 1 is the difference in total radiation received between the 2 days. Some of this difference is explained by the cloudiness on 21 December, but most may be explained by two factors. APG receives radiant energy over a longer time period (approximately 5 hours) in July than it does in December and, secondly, APG receives more direct radiation in summer than it does in winter. In this case, a surface at APG on 21 December 1983 would have received only 13% of the total radiation it would have received on 7 July 1983.

The peak value of 1.39 langleys per minute on 7 July 1983 occurred at 1:15 p.m, while the corresponding value for 21 December 1983 of 0.48 langley per minute occurred at 11:30 a.m.

## 7. DATA SUMMARY - NET RADIATION

Solar radiation measurements have been compared to various subjective estimates of that quantity. For purposes of this study the radiation measurements were reduced in three forms: an "instantaneous" measurement at the top of each hour, and the average hourly values previous to and following this time. The instantaneous measurement actually represents a subjective estimate of the average 5-minute solar radiation.

Table 7 lists the geometric means for these measurements of solar radiation for each net radiation category. The total number of occurrences do not total 214 since some occurrences of NRI equaling -1 and -2 existed. Recall that radiation data was collected near sunrise in winter months.

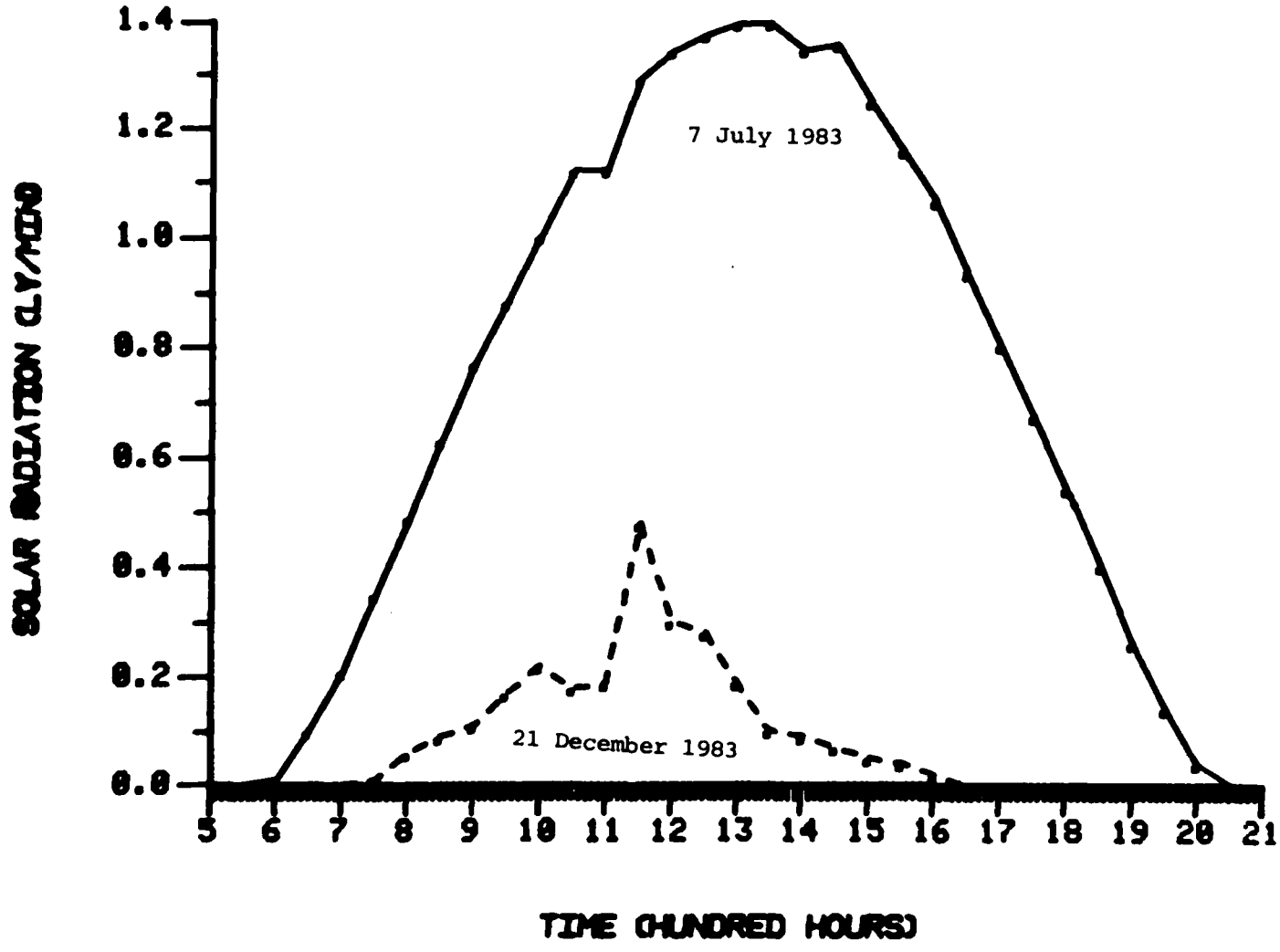


Figure 1. Measured Solar Radiation for Two Select Dates

This time period is defined as "night" by the Pasquill-Turner (P-T) System, and the stability category was often E or F. These 10 data points have been eliminated. Only Pasquill Stability Categories A through D were analyzed.

Table 7. Mean Values* of Solar Radiation for Net Radiation Categories 0 through 4

| NRI | Number of occurrences | Hourly average | Instantaneous | Number of occurrences | Hourly delay |
|---|---|---|---|---|---|
| 0 | 45 | .16 | .15 | 38 | .18 |
| 1 | 43 | .30 | .33 | 39 | .33 |
| 2 | 47 | .49 | .52 | 45 | .52 |
| 3 | 42 | .83 | .85 | 33 | .90 |
| 4 | 27 | 1.08 | 1.08 | 27 | 1.14 |
| | 204 | | | 182 | |

*Langleys per minute

Table 7 shows that the P-T net radiation index (NRI) is intrinsically correct. As the NRI increases, so do the solar radiation measurements. Note that all three measurements of solar radiation are comparable with one another.

The geometric means given in Table 7 list the approximate value for each NRI category, but it presents nothing in relation to the distribution of the solar radiation measurements about the means. Tables 8 and 9 list the joint occurrence of the NRI category and solar radiation.

Table 8. Joint Occurence of NRI and Instantaneous Radiation (204 Observations)

| | Instantaneous insolation* | | | | | |
|---|---|---|---|---|---|---|
| NRI | <.2 | .20-.39 | .40-.69 | .70-1.09 | > 1.1 | Total |
| 0 | 16.2% | 4.4 | 0 | 1.5 | 0 | 22.1 |
| 1 | 7.8 | 9.3 | 2.5 | 1.0 | 0.5 | 21.1 |
| 2 | 1.9 | 5.9 | 11.3 | 3.4 | 0.5 | 23.0 |
| 3 | 0 | 2.5 | 2.9 | 10.8 | 4.4 | 20.6 |
| 4 | 0 | 0.5 | 1.5 | 2.9 | 8.3 | 13.2 |
| | 25.9 | 22.6 | 18.2 | 19.6 | 13.7 | 100.0 |

*Langleys per minute

Table 9. Joint Occurence of NRI and Hourly Delay Radiation (182 Observations)

| | Hourly delay insolation* | | | | | |
|---|---|---|---|---|---|---|
| NRI | <.2 | .20-.49 | .50-.79 | .80-1.19 | > 1.2 | Total |
| 0 | 14.8% | 4.9 | 0.6 | 0.6 | 0 | 20.9 |
| 1 | 7.7 | 9.9 | 3.3 | 0.6 | 0 | 21.5 |
| 2 | 2.7 | 7.2 | 13.2 | 1.6 | 0 | 24.7 |
| 3 | 0 | 1.1 | 4.9 | 10.4 | 1.6 | 18.0 |
| 4 | 0 | 0.6 | 1.1 | 5.5 | 7.7 | 14.9 |
| | 25.2 | 23.7 | 23.1 | 18.7 | 9.3 | 100.0 |

*Langleys per minute

Table 8 is a comparison of the instantaneous value of the solar radiation at the same moment the meteorological observations were being made to determine NRI. Table 9 shows how well the NRI value predicts the average solar radiation over the next hour. However, the results show that the Pasquill-Turner (P-T) system did not fare well in this comparison. For instance, the sum of the observations along the diagonal for Tables 8 and 9 total 55.9 and 56.0%, or barely more than half the time. If there were a perfect relationship between these two systems of measurement, all the observations would be found along the diagonal.

## 8. DATA COMPARISON - INSOLATION PARAMETER $\Phi$

An interesting approach to estimating solar strength that relies somewhat on subjective measurements, but not as much as the P-T system, is described below. Equation 1 describes the flux density of solar energy on a horizontal surface.[4]

$$\text{Solar radiation strength} = K (1 - AN) \sin \alpha \qquad (1)$$

where,

K = proportionality factor dependent on the solar constant and atmospheric transmission (the amount of radiation reaching the earth's surface allowing for losses due to atmospheric scattering and absorption)

A = average cloud albedo (the percentage of incident radiation reflected)

N = percentage of sky covered by clouds

$\alpha$ = solar elevation angle (above the horizon)

Equation 1 applies to an area sufficiently large that the consequences of the irregular distribution of clouds are minimized. If K were assumed to be constant and an appropriate value for A chosen, such as 0.5, an insolation parameter $\Phi$ can be defined:

$$\Phi = (1 - 0.5\ N) \sin \alpha \qquad (2)$$

where,

$\Phi$ ranges between 0 and 1.

The solar elevation at any point on the earth's surface can be estimated very accurately using equation 3.

$$\sin \alpha = \sin \theta \sin \delta + \cos \theta \cos \delta \cos h \qquad (3)$$

where,

$\theta$ = latitude at the point of observation

$\delta$ = declination of the sun (angular distance north or south of the celestial equator)

h = hour angle of the sun (angle through which the earth must turn to bring the meridian of the observation point directly under the sun)

$\delta$ varies between 23° 27' at the summer solstice (22 June) and -23° 27' at the winter solstice (22 December) and is dependent upon geographical location. The hour angle varies by 15° for each hour difference from true solar noon, at which time it is zero. Thus, the insolation parameter $\Phi$ can be determined with the knowledge of one meteorological observation, cloudiness.

Comparisons of the insolation parameter with measured values of instantaneous solar radiation are shown in Figure 2. Each dot represents an occurrence. The solid line represents the linear regression line for this comparison. The dashed lines represent the 95% confidence interval; i.e., any data point chosen at random has a 95% probability of lying between these lines. The coefficient of determination, $r^2$, for a set of data represents a measure of the degree of relationship between variables. If there were a perfect correlation between the data, r would equal 1.0, and the data would all lie along one line. Note that the linear regression line does not really adequately describe the data. The $r^2$ value from the data in Figure 2 is 0.696.

Figure 2 represents a linear regression of $\Phi$ and solar radiation measurements. A linear regression is a first degree polynomial fit. Increasing the degree of the polynomial regression usually increases $r^2$, the coefficient of determination. However, for the data plotted in Figure 2, $r^2$ for a second degree polynomial fit had the value .703, essentially the same as the linear (first degree) regression. The data was too scattered to properly fit an equation that can be used for prediction purposes, but the $r^2$ value showed there is a strong relationship between $\Phi$ and this measurement of solar radiation.

To determine the effect the albedo had on the relationship between $\Phi$ and solar radiation, the value for A in equation 1 was varied. Values between 0.4 and 0.6 were chosen. Although the linear regression equations changed, no real differences in correlation resulted from changing the albedo value. For example, $r^2$ had the values .682 and .697 for A = 0.4 and A = 0.6, respectively.

To illustrate regression analysis as a prediction tool, Figure 3 lists measured radiation and the predicted radiation using equation 4, the linear regression equation derived from Figure 2.

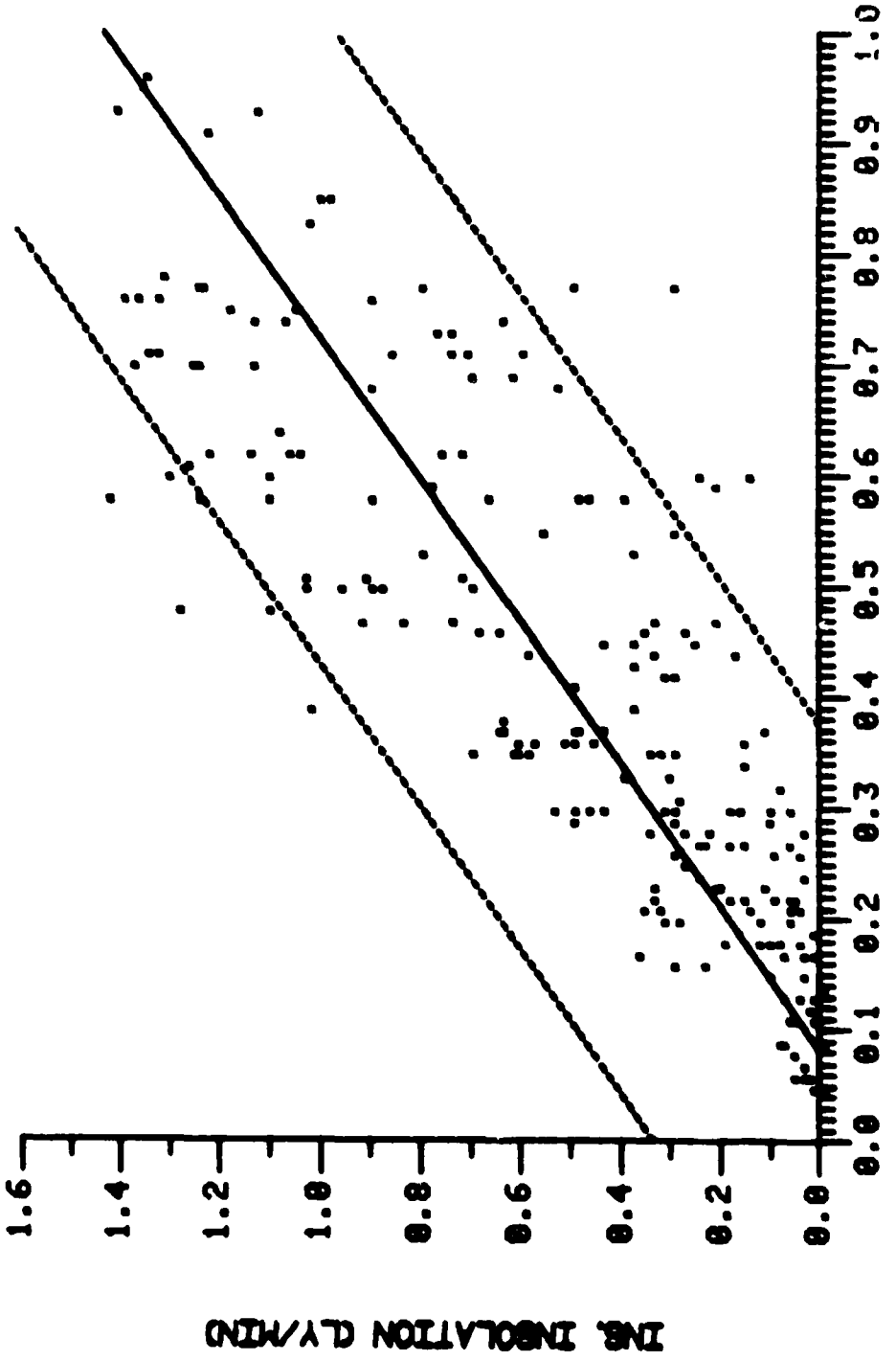


Figure 2. Linear Regression of Φ and Instantaneous Solar Radiation (Albedo = 0.5)

$$\text{Solar radiation (ly/min)} = -.1255 + 1.545\ \Phi \qquad (4)$$

where $\Phi$ is defined in equation 2.

Figure 3 shows the comparisons of equation 4 with the instantaneous solar radiation measurement taken at same time of day the cloudiness was estimated on 7 July and 21 December. Figure 3 shows that equation 4 fits well with the 21 December data, but not the 7 July data. The general shape of the 7 July prediction curve is correct (the line predicts an increase in solar radiation until 12 noon to 1 p.m, then falls off), but the magnitude of the estimate does not correspond to the measured value. More than anything else, this may point out the problem with comparing the measurement of solar radiation at a point with an insolation parameter ($\Phi$) intended for a sufficiently large area. Additionally, comparing the instantaneous (5-minute average) measurement of solar radiation is also risky. For example, even though much of the sky is obscured by cloud, the pyranometer may be "seeing" radiation through small openings, which would sense more radiation than the area in this vicinity. A time-average value of the solar radiation should provide more accurate estimates.

Figure 4 shows the correlation between the insolation parameter $\Phi$ and the average radiation over the next 60 minutes, i.e., how well $\Phi$ can be used to predict the upcoming solar radiation. Note that the 95% confidence interval is narrower than that in Figure 2, indicating a better fit. In fact, the $r^2$ value associated with Figure 4 is .792. This comparison would indicate that a time-average of the solar radiation is more reasonable than an instantaneous measurement.

Figure 5 has been included to show the effects of changing the degree of the polynomial for the regression analysis. Note the change in slope of the regression line at the bottom left of the graph, the area where the observations are most cluttered. The $r^2$ value for Figure 5 is .798, and the regression equation (solid line on Figure 5) can be described by equation 5.

$$\text{Solar radiation (ly/min)} = .1177 - .9282\ \Phi + 7.486\ \Phi^2 - 8.461\ \Phi^3 + 3.194\ \Phi^4 \qquad (5)$$

Changing the albedo value in equation 1 again had little effect on the correlation of these observations.

The insolation parameter $\Phi$ is essentially an observation at a single moment in time. $\Phi$ will change even in short time spans because the solar elevation constantly changes. In addition, the cloud cover can often change rapidly. To determine these possible effects, $\Phi$ could be averaged over short time periods such as 1 hour. For these purposes $\Phi_p$ will be the insolation parameter averaged over a period of 1 hour previous to the solar radiation measurement.

For example, Figure 6 shows the relationship between $\Phi_p$ and the instantaneous measurement of insolation. As noted earlier, the instantaneous measurement of radiation is not always a good indicator of the amount of radiation the general area is receiving. Note that there is a correlation between the two measurements, but you would not feel very confident predicting the instantaneous radiation using $\Phi_p$.

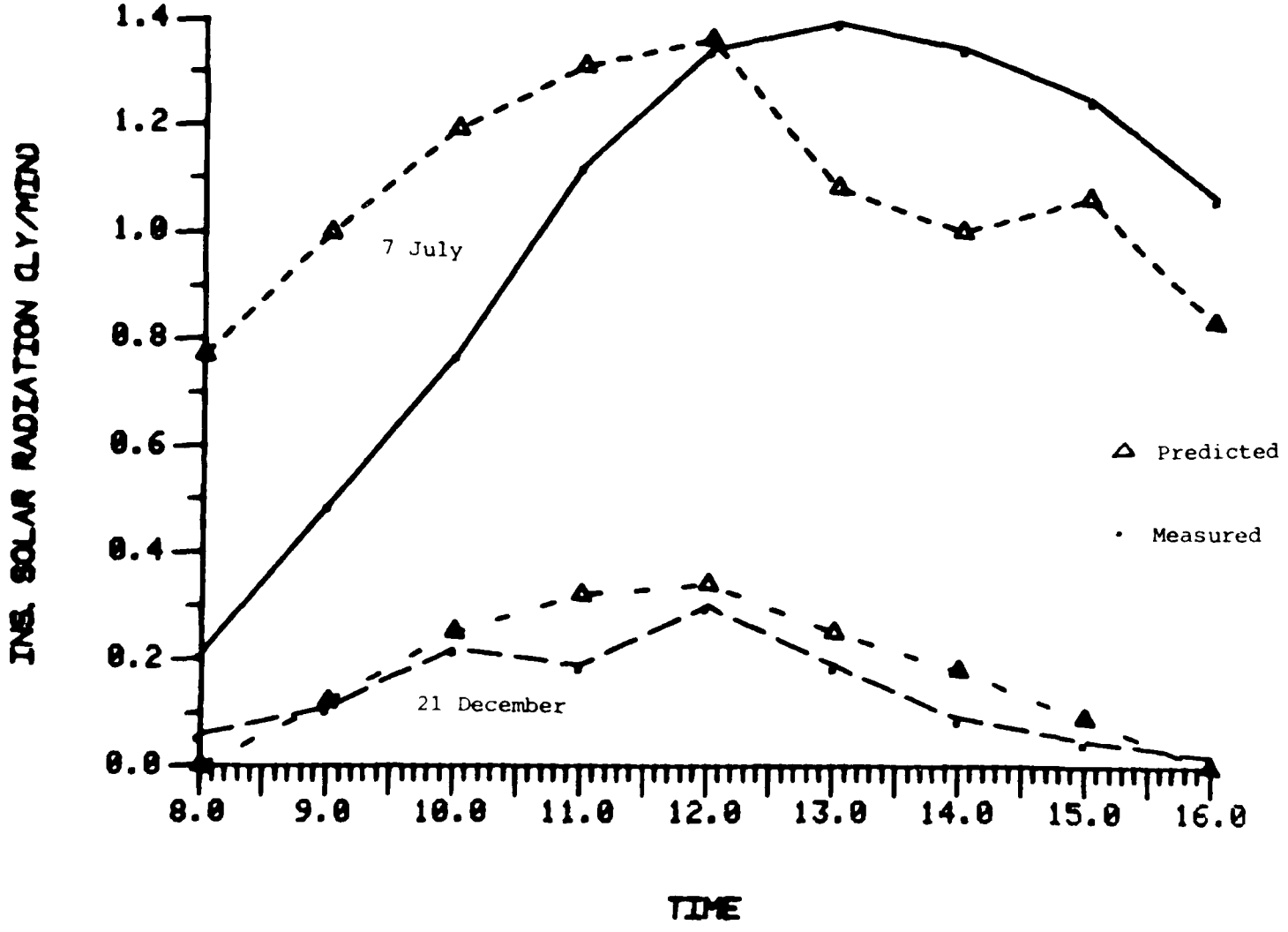


Figure 3. Comparison of Measured and Predicted Solar Radiation for Two Select Dates

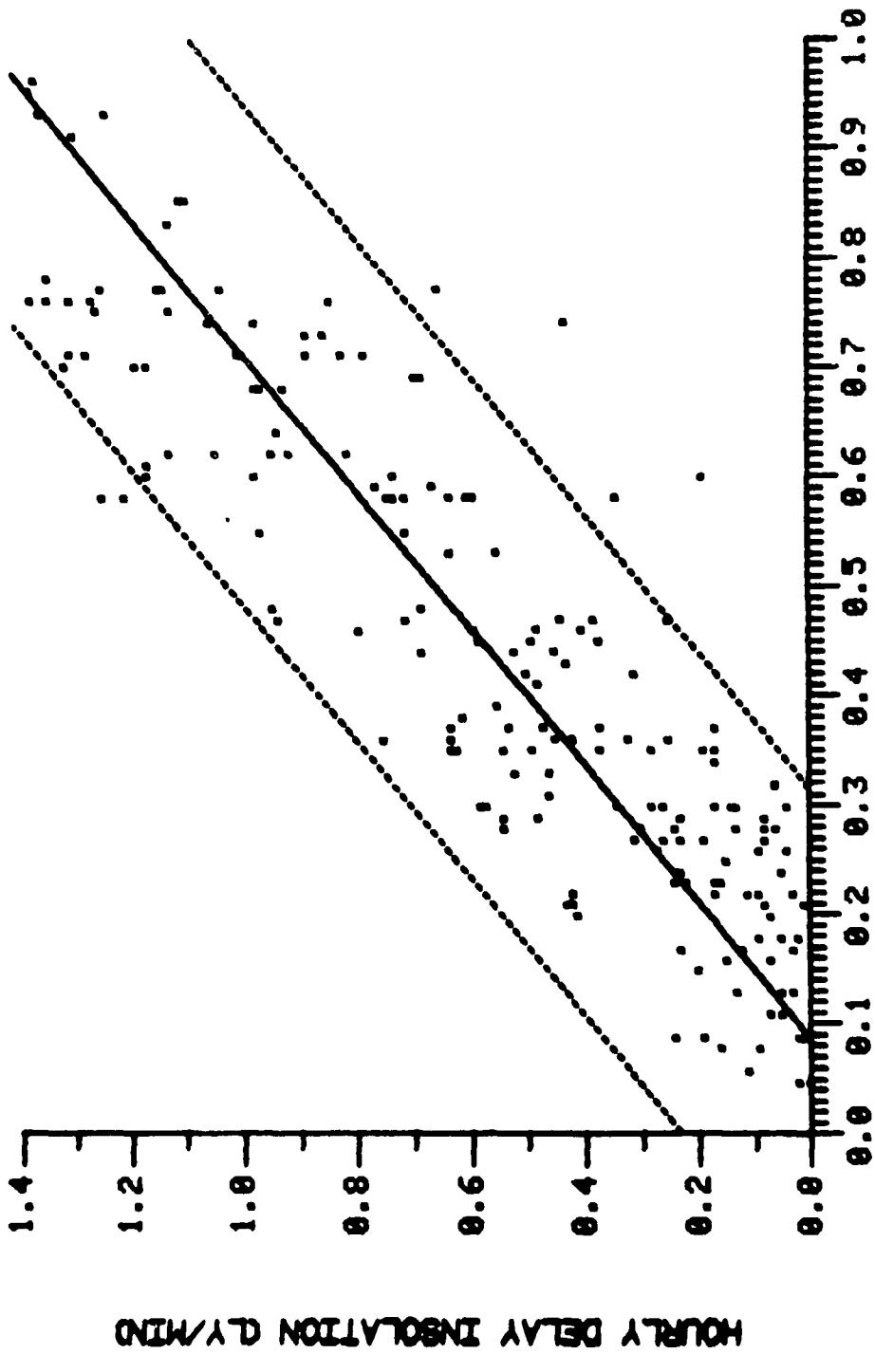


Figure 4. Linear Regression of Φ and Hourly Delay Solar Radiation (A = 0.5)

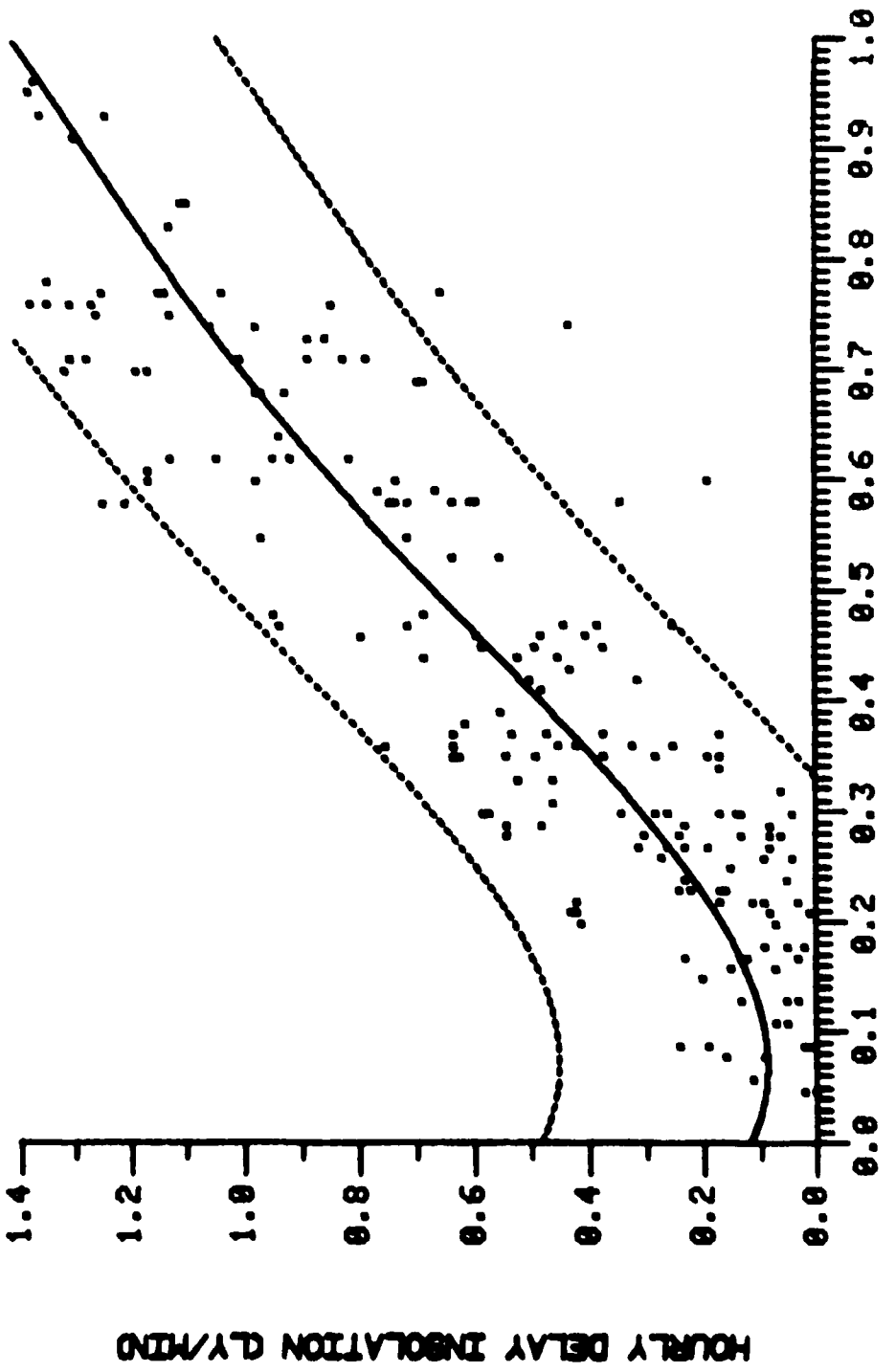


Figure 5. Four-Degree Regression of Φ and Hourly Delay Solar Radiation (A = 0.5)

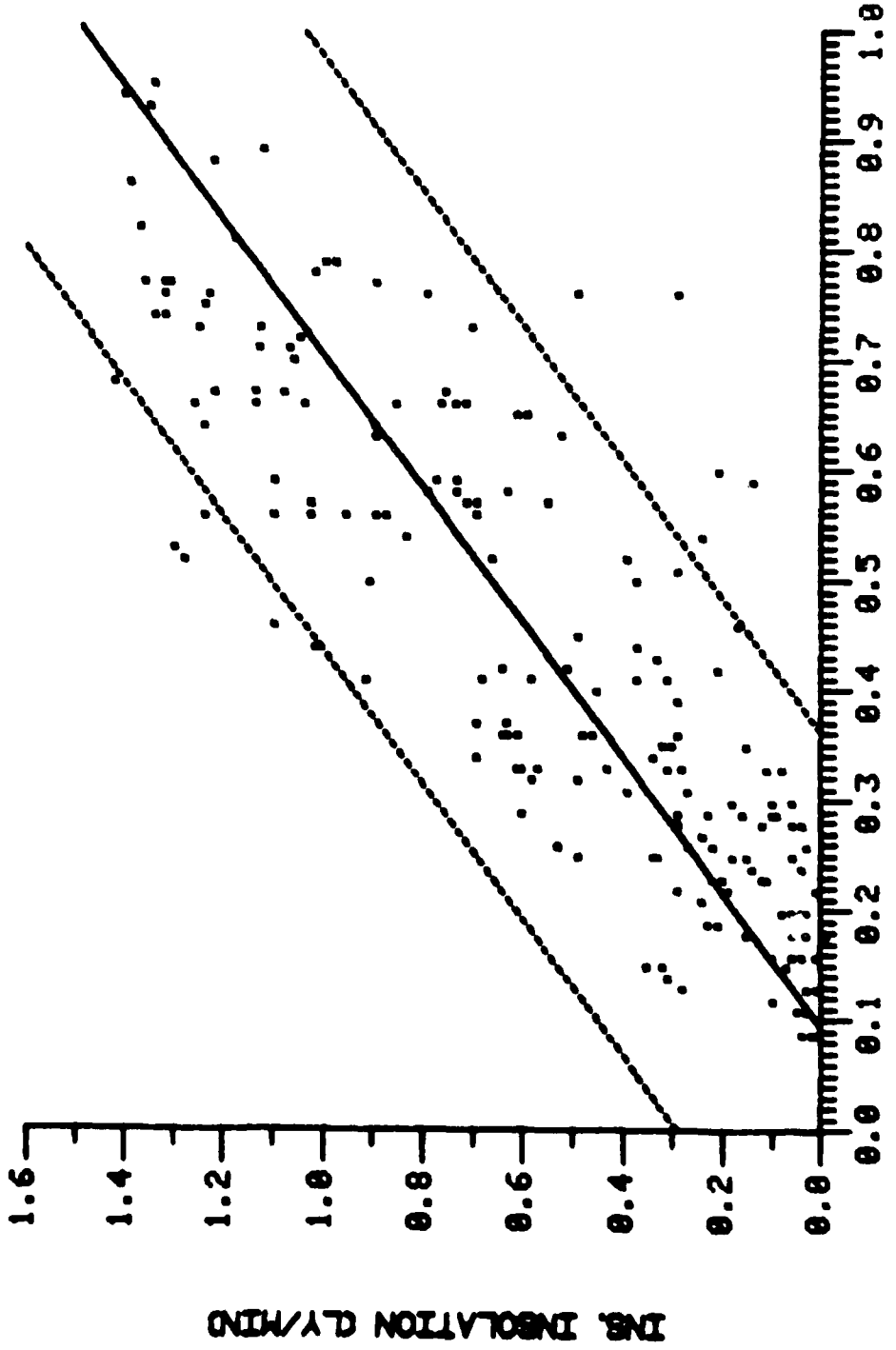


*Figure 6. Linear Regression of $\Phi_p$ and Instantaneous Solar Radiation (A = 0.5)*

Using $\Phi_p$ to predict the average radiation should provide more accurate estimates. Figure 7 shows the relationship between the insolation parameter averaged over the same time period as the solar radiation. The relationship is more accurate than that evident from the measurement of the instantaneous radiation. The correlation of coefficient for the data used in Figure 7 is .772.

Once again employing $\Phi_p$ as a predictor, Figure 8 shows the effects of $\Phi_p$ in estimating the time-lag solar radiation. Here $\Phi_p$ is the average insolation parameter over a given hour, and the radiation measurement is the average value for the next hour. This relationship provided the best correlation, as determined by the correlation coefficient $r^2$, of any variables analyzed for this study. The corresponding $r^2$ value for Figure 8 is .800. It is interesting to note that the $r^2$ for this same set of observations is .813 when the albedo is defined to be 0.6. Figure 8 shows that the insolation parameter seems to be more accurate when it is averaged over a short time period (~ 1 hour) and used as a predictor instead of a measure of the current conditions.

Comparisons of the hourly delay insolation with two insolation parameters, $\Phi$ and $\Phi_p$, are shown in Figure 9. The measured radiation measurements are the same as in Figure 3. For the 7 July case, $\Phi_p$ provides the better descriptor of the actual radiation, but it overestimates the radiation until about 1 p.m, after which time it underestimates it. However, $\Phi$ proved to be the better indicator of solar radiation in the 21 December case. The $\Phi$ curve follows the measured radiation curve closely. Note that for the summer case both predictors overestimate the measured radiation for the first half of the day and underestimate it for the second half, and the reverse is true for the winter case. There is no apparent reason for this pattern.

Table 10 summarizes the different ways in which the insolation parameter and solar radiation were compared, along with the associated correlation coefficient.

Table 10. Summary of Comparisons between the Insolation Parameter and Measured Solar Radiation

| Insolation parameter | Albedo | Solar radiation | $r^2$ (correlation coefficient) |
|---|---|---|---|
| $\Phi$ | 0.5 | Instantaneous | .696 |
| $\Phi_p$ | 0.5 | Instantaneous | .724 |
| $\Phi_p$ | 0.5 | Average hourly | .772 |
| $\Phi$ | 0.5 | Hourly delay | .792 |
| $\Phi_p$ | 0.5 | Hourly delay | .800 |
| $\Phi_p$ | 0.6 | Hourly delay | .813 |

Table 10 clearly shows the benefits of time-averaging both the insolation parameter and solar radiation to determine the best correlation. Also shown are the benefits of using $\Phi$ as a predictor instead of a measurement of the current conditions.

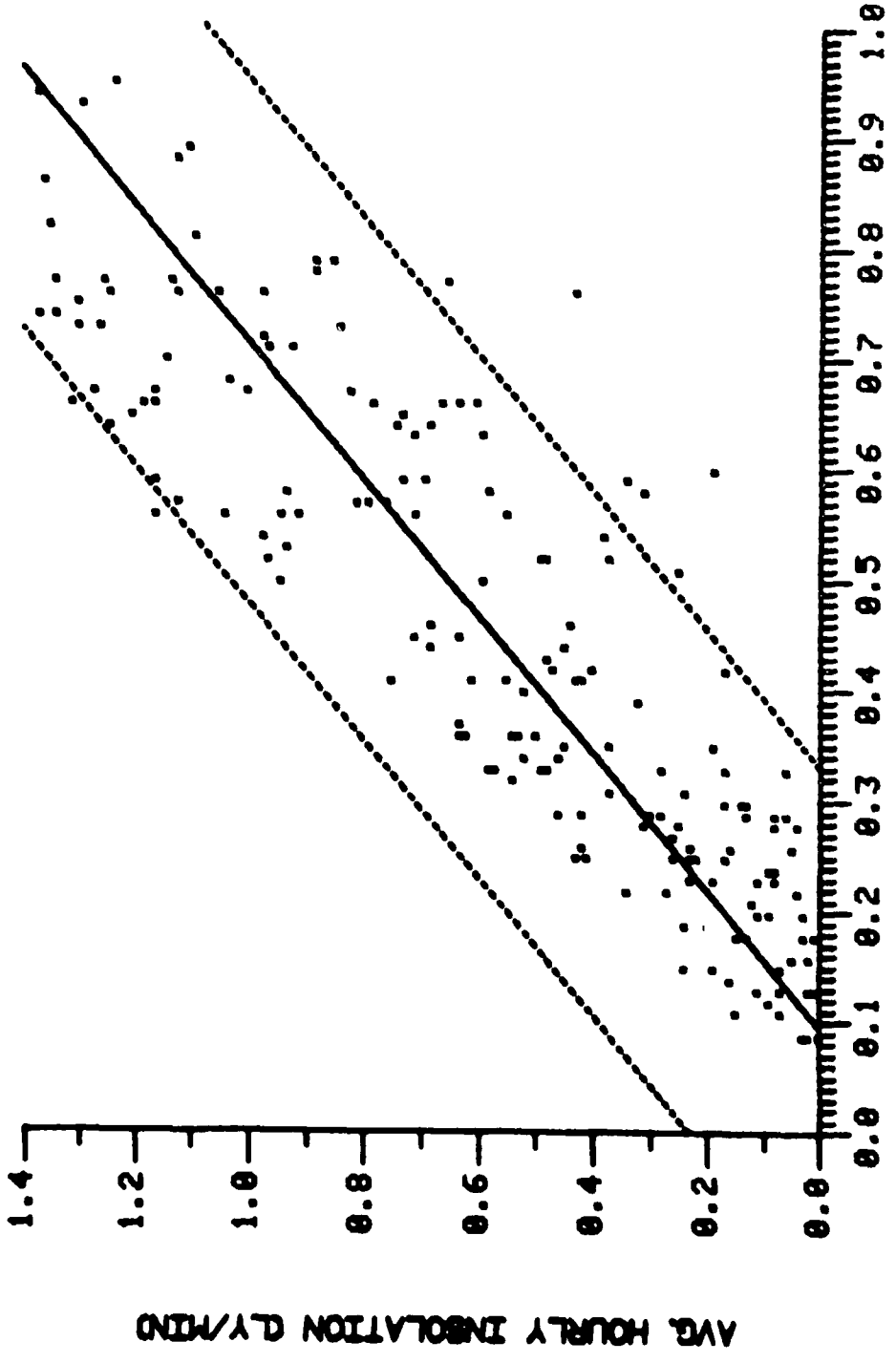


Figure 7. Linear Regression of $\Phi_p$ and Average Hourly Solar Radiation (A = 0.5)

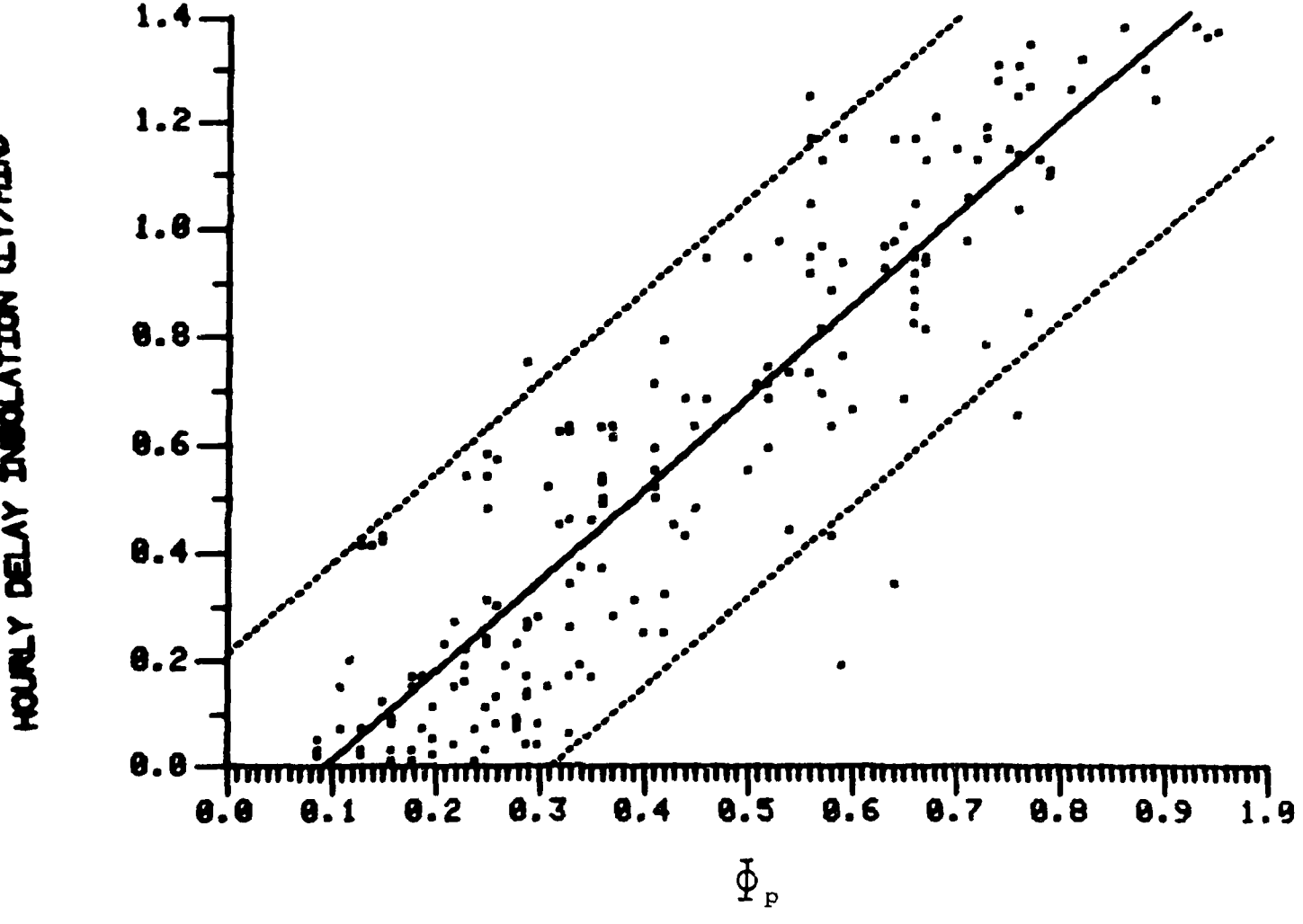


Figure 8. Linear Regression of $\Phi_p$ and Hourly Delay Solar Radiation (A = 0.5)

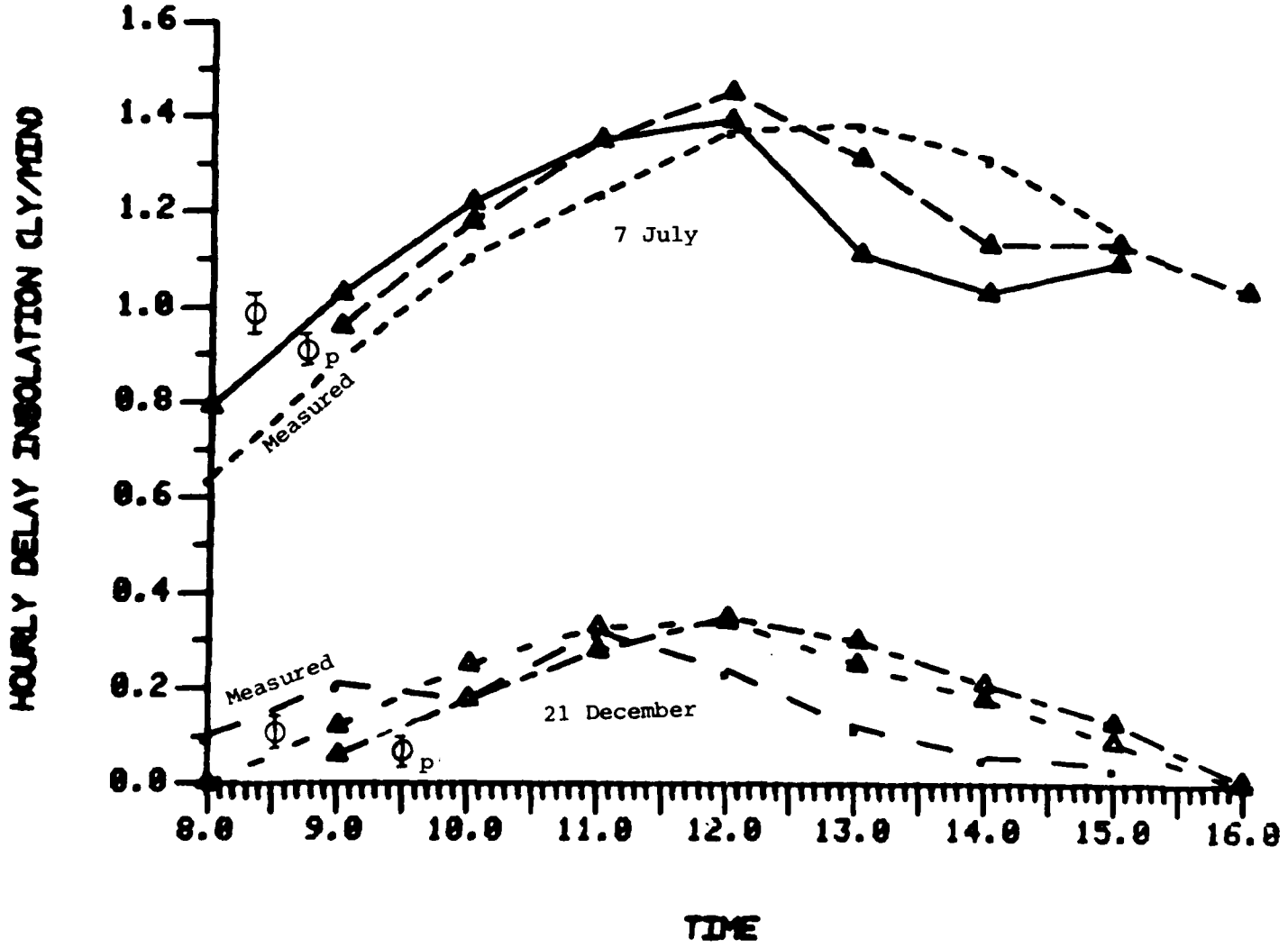


Figure 9. Comparison of $\Phi$ and $\Phi_p$ with Hourly Delay Solar Radiation

There are two possible reasons that the correlations summarized in Table 10 are not higher. First, all solar radiation measurements were made with one stationary pyranometer, essentially a fixed point. The insolation parameter $\Phi$ is intended to estimate the strength of solar radiation for a general area. The problem of cloudiness over a general area and that at a point were discussed previously. There is no doubt that averaging at least two measurements of solar radiation, adequately spaced, would improve this relationship. Secondly, K is not really constant as assumed in equation 1. K is a function of the solar constant, which is quite constant, and atmospheric transmission, which fluctuates with time. The amount of scattering and absorption varies with sky conditions, including synoptic (large-scale) weather patterns and atmospheric pollutants.

Another way to determine the relationship between two parameters is by using the joint occurrence table, showing the frequency of occurrence of one parameter with another. Table 11, which categorizes the same observations used in Figure 2, is an example. Table 11 details how the sum of all occurrences of one parameter corresponds with the other. For example, 18.7% of all observations occurred with $.30 \leq \Phi < .49$ and $.30 \leq SR \leq .69$. Also, when $.30 \leq \Phi \leq .49$, 65.4% of the solar radiation measurements fell between .30 and .69 $\left(\frac{18.7}{28.6}\right) = .654$ .

Table 11. Joint Occurence of Insolation Parameter $\Phi$ and Instantaneous Solar Radiation
(214 observations, A = 0.5)

| | Instantaneous solar radiation (ly/min) | | | | |
|---|---|---|---|---|---|
| $\Phi$ | < .3 | .30-.69 | .70-1.09 | > 1.1 | |
| <.3 | 29.9 | 5.6 | 0 | 0 | 35.5 |
| .30-.49 | 6.1 | 18.7 | 3.3 | 0.5 | 28.6 |
| .50-.69 | 1.4 | 4.7 | 9.8 | 3.3 | 19.2 |
| >.70 | 0 | 1.8 | 5.6 | 9.3 | 16.7 |
| | 37.4 | 30.8 | 18.7 | 13.1 | 100.0 |

Tables 12 through 15, corresponding to Figures 4, 6, 7, and 8, respectively, are shown.

Table 12. Joint Occurrence of Insolation Parameter $\Phi$ and Average Hourly Delay Radiation (187 observations, A = 0.5)

| | Average hourly delay radiation (ly/min) | | | | |
|---|---|---|---|---|---|
| $\Phi_p$ | <.3 | .30-.69 | .70-.99 | >1.0 | |
| <.3 | 27.3 | 5.3 | 0 | 0 | 32.6 |
| .30-.49 | 7.5 | 20.9 | 2.7 | 0 | 31.1 |
| .50-.69 | 0.5 | 4.3 | 9.1 | 3.2 | 17.1 |
| > .70 | 0 | 1.1 | 3.7 | 14.4 | 19.2 |
| | 35.3 | 31.6 | 15.5 | 17.6 | 100.0 |

Table 13. Joint Occurrence of Insolation Parameter $\Phi_p$ and Instantaneous Solar Radiation (187 observations, A = 0.5)

| | Instantaneous solar radiation (ly/min) | | | | |
|---|---|---|---|---|---|
| $\Phi_p$ | <.3 | .30-.69 | .70-1.09 | >1.1 | |
| <.3 | 26.2 | 7.5 | 0 | 0 | 33.7 |
| .30-.49 | 5.3 | 16.6 | 2.7 | 0 | 24.6 |
| .50-.69 | 1.6 | 5.3 | 13.9 | 4.8 | 25.6 |
| > .70 | 0 | 1.1 | 4.8 | 10.2 | 16.1 |
| | 33.1 | 30.5 | 21.4 | 15.0 | 100.0 |

Table 14. Joint Occurrence of Insolation Parameter $\Phi_p$ and Average Hourly Radiation (187 observations, A = 0.5)

| | Average hourly radiation (ly/min) | | | | |
|---|---|---|---|---|---|
| $\Phi_p$ | <.3 | .30-.69 | .70-1.09 | >1.1 | |
| <.3 | 28.9 | 4.8 | 0 | 0 | 33.7 |
| .30-.49 | 5.3 | 18.2 | 1.1 | 0 | 24.6 |
| .50-.69 | 1.1 | 7.5 | 11.8 | 5.3 | 25.7 |
| > .70 | 0 | 1.1 | 5.3 | 9.6 | 16.0 |
| | 35.3 | 31.6 | 18.2 | 14.9 | 100.0 |

Table 15. Joint Occurrence of Insolation Parameter $\Phi_p$ and Average Hourly Delay Radiation (187 observations, A = 0.5)

| $\Phi_p$ | Average hourly delay radiation (ly/min) <.3 | .30-.69 | .70-1.09 | >1.1 | |
|---|---|---|---|---|---|
| <.3 | 27.3 | 6.0 | 0.5 | 0 | 33.8 |
| .30-.49 | 7.0 | 16.0 | 1.6 | 0 | 24.6 |
| .50-.69 | 0.5 | 4.8 | 16.0 | 4.3 | 25.6 |
| > .70 | 0 | 0.5 | 3.2 | 12.3 | 16.0 |
| | 34.8 | 27.3 | 21.3 | 16.6 | 100.0 |

Had all the observations been located along the diagonal running from top left to bottom right in each table, this method of comparison would have implied a "perfect" relationship between the variables. The sum of the observations along the diagonals ranged from 66.9% (Table 13) to 71.6% (Table 15) and 71.7% (Table 12). The measurement of insolation in the form of hourly averages was found to have the highest percentage of observations along the diagonals, while the instantaneous measures provided the smallest percentage of observations along the diagonals.

Similar to the results from the regression analyses discussed earlier, the albedo value in Tables 11-15 had little effect on the relationship between the insolation parameter $\Phi$ and the insolation measurements.

## 9. DATA COMPARISON - SMITH ALGORITHM

For comparative purposes, a previous study of solar radiation has been included. Smith developed an algorithm (Figure 10) for determining the Pasquill Stability Parameter from the direct measurement of solar radiation and wind.[5] Figure 10 includes the stability determination for the daytime only. Smith included a provision for nighttime stability as determined by the upward heat flux at the surface, but this has not been included since nighttime measurements are not used in this study.

The most noticeable feature of Figure 10 is the determination of stability on a continous scale. Recall that the P-T system categorized the daytime stability parameter into one of four distinct values ranging from A to D. The Smith Algorithm allows split categories. For example, the stability parameter 2.2 is towards the more unstable end of category C. (These split categories are important in determining $\sigma_z$ (x), the vertical standard deviation of the chemical cloud, a measure of the vertical growth. This parameter determines the downwind concentration or dosage of the chemical cloud.)

Two patterns are evident in Figure 10. As the solar radiation increases, assuming a constant wind speed, the stability parameter becomes more unstable. Secondly, keeping solar radiation constant and increasing the wind speed pushes the stability parameter toward neutral, the most stable condition possible during the daytime. These same patterns existed in the P-T stability algorithm (Table 3).

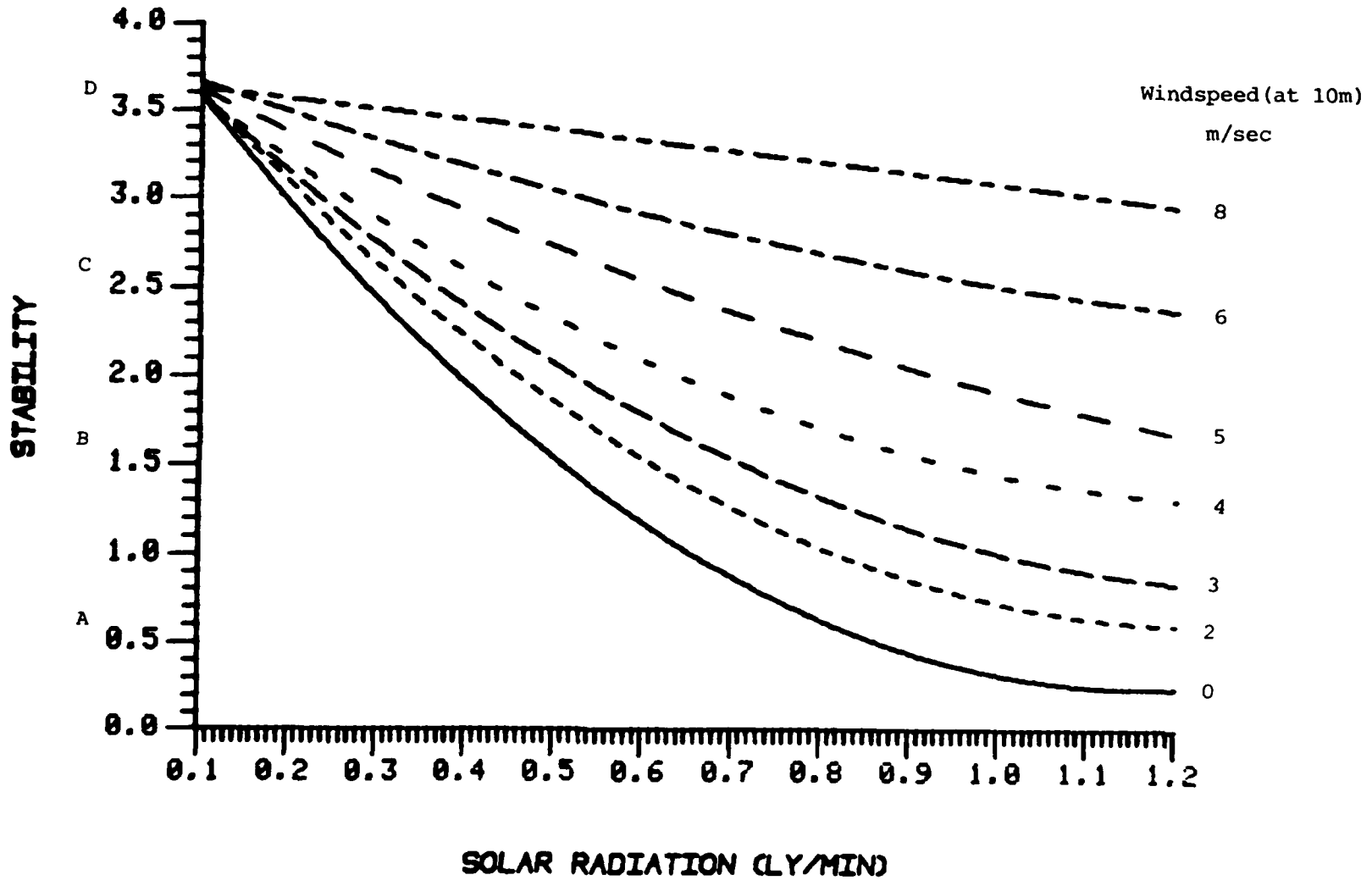


Figure 10. Smith Nomogram for the Determination of Pasquill Stability Parameter

Note that the neutral stability is assigned the value 3.6 in Figure 10. If numerical values were to be assigned to the P-T categories, A would equal 1.0, B = 2.0, C = 3.0, and D (neutral) = 4.0. The corresponding values from Figure 10 are 0.6, 1.6, 2.6, and 3.6, respectively, which represent the center of each P-T stability category. Thus, to compare stability parameters, add 0.4 to the Smith value to obtain the P-T stability parameter.

Smith also included a provision for determining stability based on the upward heat flux (UHF), the transfer of heat from the earth's surface (see Section 2). The UHF could be measured directly or it could be estimated using equation 5 and, if measured directly, could be used for a nighttime stability indicator.[5]

$$UHF = 0.4\ (SR - .1433) \qquad (6)$$

where, UHF and solar radiation have units (ly/min).

Assuming the measurement of UHF, equation 5 allows the calculation of stability on a continuous, daily scale. Neither the UHF scale nor the nighttime stability curves are shown in Figure 10.

Table 16 lists the P-T stability category as determined using the solar radiation data summarized in this report. Table 16 considers only discrete stability parameters, since the stability parameter was not recorded on a continuous scale. The table includes interpolations where data was not recorded. The solar radiation measurement represents a 1-hour time average. Table 16, then, summarizes the average hourly radiation with the corresponding P-T stability index as determined by the cloud cover, cloud height, and solar elevation.

Table 16. Pasquill Stability Category Based on the Direct Measurement of Solar Radiation

| | Solar radiation (ly/min) | | | | | | | | | | |
|---|---|---|---|---|---|---|---|---|---|---|---|
| wind speed (m/sec) | 0 | .1 | .2 | .3 | .4 | .5 | .6 | .7-.9 | 1.0 | 1.1 | > 1.2 |
| 0 | D | C-D | C | B | B | A-B | A | A | A | A | A |
| 1 | D | D | C | B | B | B | B | B | B | B | A |
| 2 | D | D | D | C-D | C | C | B | B | B | B | B |
| 3 | D | D | D | C-D | C | C | C | C | B-C | B | B |
| 4 | D | D | D | D | D | | C | | | | |
| 5 | D | D | D | | | | | | | | |
| > 6 | D | D | D | | | | | | | | |

Table 16 lists the most frequent occurrence of the stability index for the corresponding wind speed and solar radiation measurements. Some split categories existed and are denoted by a (-).

The same general trends shown in Figure 10 are seen in Table 16: (a) increasing the solar radiation as the wind speed remains constant decreases the stability parameter (more unstable) and (b) increasing the wind speed as the solar radiation remains constant increases the stability parameter (toward neutral).

The greatest range of stability occurred when the anemometer recorded calm conditions. The stability parameter varied from D to A over a range of only 0.6 ly/min. It is interesting to note that the occurrence of stability A was virtually confined to calm winds. Outside the zero wind category, stability A appears on Table 16 only when the wind speed equaled 1 m/sec and solar radiation measured at least 1.2 ly/min. Note that repetition allowed the combination of some radiation categories, i.e., .7-.9 and > 1.2 ly/min.

In general, the data in Table 16 compares favorably with that in Figure 10. For calm winds, the stability parameters match except for the 0.4 and 0.6 insolation categories, where in Table 16 one stability category closer to the unstable end is predicted. For a 2-m/sec wind speed, the curves agree quite well except in the range .85-1.00 ly/min, where in Figure 10 an A stability is predicted while in Table 16 B stability is indicated. At the 3-m/sec wind, the curves agree up to 0.5 ly/min insolation, but beyond this value (Figure 10) a more unstable category is predicted. Finally, in Table 16 a neutral stability category up to at least 0.4 ly/min is predicted, while in Figure 10 a neutral category only to approximately 0.2 ly/min is indicated. Due to insufficient data involving higher wind speeds, comparisons between the two systems could not be made. However, for all observations where comparisons could be made, the two systems never differed by more than one stability category.

One point concerning this comparison should be emphasized. The data used to generate Table 16 was collected in the vicinity of trees and buildings near an inlet of the Chesepeake Bay. The wind barriers and large water body affect both the local circulation of winds and the surface heating (not how much insolation received per se, but how much retained), the two governors of atmospheric stability. On the other hand, Figure 10 applies to open terrain. Therefore, Table 16 may have to be revised slightly if it is to apply to a generalized, mid-latitude temperate climate.

Table 17 has been included for comparative purposes, displaying the Pasquill stability category as a function of the insolation parameter $\Phi_p$ and wind speed. Table 17 was developed from the same observations as Table 16, and $\Phi_p$ represents a 1-hour average for the same observations. A direct comparison to Figure 10 is not possible, but the same trends of stability found in Figure 8 and Table 3 also exist here.

Table 17. Pasquill Stability Parameter Based on $\Phi_p$

| wind speed (m/sec) | $\Phi_p$ (dimensionless) 0-0.2 | .3 | .4 | .5 | .6 | .7 | > .80 |
|---|---|---|---|---|---|---|---|
| 0 | D | C | B | A | A | A | A |
| 1 | D | C | B | B | B | A | A |
| 2 | D | C | C | C | B | B | A |
| 3 | D | C | C | C | C | B | |
| 4 | D | D | C | | | | |
| 5 | D | D | | | | | |
| > 6 | D | D | | | | | |

## 10. CONCLUSIONS

Two subjective estimates of solar radiation have been compared with pyranometer measurements. Both the P-T and insolation parameter $\Phi$ methods displayed a reasonably good fit with the field data. In comparing the two subjective estimates, the insolation parameter $\Phi$ was judged to perform better than the P-T system.

The relationship between all variables improved when time-averaged quantities were considered.

Three factors negatively influenced the performance of the insolation parameter $\Phi$:

- The proportionality factor dependent on atmospheric transmission is not constant. The amount of solar radiation allowed through the atmosphere can vary greatly over the range of synoptic (large-scale) weather conditions.

- The average cloud albedo used does not apply to all cloud types.

- The solar radiation measurements were collected at a single point. Fluctuations in insolation due to irregular cloud distributions can be expected at a point, which may not accurately describe the solar radiation being received over the general area. It is reasonable to expect these fluctuations to be smoothed through the averaging of insolation at several, well-spaced points.

Several factors may have negatively influenced the performance of the P-T system:

- Cloud cover and cloud height measurements were made subjectively. Cloud height was estimated based on the identity of cloud type. However, several cloud types are similar in appearance and difficult to distinguish. In addition, such atmospheric conditions as haze can make it difficult to quantify cloud cover and height.

- There is reason to believe that the anemometer recordings of wind speed are low, i.e., the actual wind speeds were higher than that recorded.

- The solar radiation measurements were collected at a single point, while the P-T system defines atmospheric stability for a generalized area. There is no doubt this accounts for some error in comparison of the two quantities.

Algorithms have been provided that select the Pasquill Stability Category based on the direct measurement of solar radiation. These algorithms eliminate the need to subjectively estimate insolation. Where the direct measure of solar radiation is not possible, the insolation parameter $\Phi$ and P-T systems have been shown to be adequate methods for characterizing solar radiation.

The ultimate use of all atmospheric stability predictors is to estimate the dispersion rates of vapors, aerosols, and/or smokes under those meteorological conditions. It is recognized that this study does not predict the behavior of a chemical cloud introduced to the atmosphere, but it provides a slightly simpler method to determine atmospheric stability.

## 11. RECOMMENDATIONS

Data from time periods other than those recorded here should be collected and analyzed to determine if the results presented in this study contrast significantly. It is expected that the average solar radiation measurements associated with stability category D will prove to be higher when more data has been collected. In this study, most incidences of stability D occurred near sunrise or sunset, when insolation had to be low. However, stability D can also occur during miday under heavy cloud cover. The solar radiation reaching the surface should be higher under these circumstances. Data should be collected using at least two, well-spaced pyranometers.

Data should be reduced automatically. A significant portion of time for this study was spent reducing data.

Measurements of surface heat flux could be used to determine its relationship to surface insolation. These measurements could then be used to determine atmospheric stability during the daytime or nighttime. Solar radiation measurements, obviously, can only be used to determine daytime stability.

Blank

## LITERATURE CITED


1. Turner, D. Bruce. Relationship Between 24-Hour Mean Air Quality Measurements and Meteorology Factors at Nashville, Tennessee. J. Air Pollut. Control Assoc. 11 (10), 483-489 (1961).

2. Smithsonian Meteorological Tables, Sixth Revised Edition. Smithsonian Institution. 1971.

3. Federal Meteorological Handbook No. 1 National Oceanic and Atmospheric Administration. U.S. Department of Commerce.

4. Ludwig, F.L., and Dabberdt, Walter F. Comparison of Two Practical Atmospheric Stability Classification Schemes in an Urban Application. J. Appl. Meteorol. 15, 1172 (1976).

5. Smith, F.B. A Scheme for Estimating the Vertical Dispersion of Plumes from a Source Near Ground Level. Proc. Third Meeting Expert Panel on Air Pollution Modeling. NATO Committee on Challenges of Modern Society, XVII-1 to XVII-14. 1972.

END

DATE

FILMED

JAN

1988